

# A MODEL FOR COUPLED MECHANICAL AND HYDRAULIC BEHAVIOUR OF A ROCK JOINT

T. S. NGUYEN<sup>1</sup> AND A. P. S. SELVADURAI<sup>2\*</sup>

<sup>1</sup>Atomic Energy Control Board, 280 Slater, Ottawa, Canada K1G 0R9

<sup>2</sup>McGill University, 817 Sherbrooke West, Montreal, Canada, H3A 2K6

## SUMMARY

Constitutive laws for rock joints should be able to reproduce the fundamental mechanical behaviour of real joints, such as dilation under shear and strain softening due to surface asperity degradation. In this work, we extend the model of Plesha to include hydraulic behaviour. During shearing, the joint can experience dilation, leading to an initial increase in its permeability. Experiments have shown that the rate of increase of the permeability slows down as shearing proceeds, and, at later stages, the permeability could decrease again. The above behaviour is attributed to gouge production. The stress-strain relationship of the joint is formulated by appeal to classical theories of interface plasticity. It is shown that the parameters of the model can be estimated from the Barton-Bandis empirical coefficients; the Joint Roughness Coefficient (JRC) and the Joint Compressive strength (JSC). We further assume that gouge production is also related to the plastic work of the shear stresses, which enables the derivation of a relationship between the permeability of the joint and its mechanical aperture. The model is implemented in a finite element code (FRACON) developed by the authors for the simulation of the coupled thermo-hydraulic-mechanical behaviour of jointed rock masses. Typical laboratory experiments are simulated with the FRACON code in order to illustrate the trends predicted in the proposed model. © 1998 by John Wiley & Sons, Ltd.

Int. J. Numer. Anal. Meth. Geomech., Vol. 22, 2948 (1998)

(No. of Figures: 16 No. of Tables: 0 No. of Refs: 39)

Key words: hydraulic behaviour; joint; mechanics of joint; joint degradation; joint elements; interface mechanics

## INTRODUCTION

Discontinuities in rock masses, which shall be referred to as 'joints' in this paper, constitute planes of weakness in the rock mass from the point of view of its mechanical behaviour. Under external loads, sliding along the joints is likely to occur. Due to the presence of asperities at the joint surfaces, dilation usually accompanies the shearing process, leading to an increase in the joint aperture. As a consequence, the joint becomes more permeable. The asperities of the joint walls have finite strength. Mechanical degradation of these asperities occurs during shear, and the dilation of the joint will diminish at the later stages of the shearing process. During this process, gouge material is being produced by the damage of the asperities and the accumulation of the gouge material can result in the reduction of flow in the joint. The very limited number of

\*Correspondence to A. P. S. Selvadurai, McGill University, 817 Sherbrooke Street West, Montreal, Canada, H3A 2K6

experiments<sup>24</sup> which investigate the effects of shear on joint permeability show that as shearing proceeds, the permeability decreases as a result of gouge production.

Patton<sup>5</sup> performed experiments on artificial joints with regular  $\bar{O}$ -saw-tooth $\bar{O}$  shapes moulded out of plaster of Paris. He proceeded to propose a bilinear model of a shear strength criterion; at low normal stress, the joint shows dilation during shear due to overriding of the asperities; at high normal stress, shear through the asperities occurs and limited dilation is observed. Ladanyi and Archambault,<sup>6</sup> Jaeger,<sup>7</sup> Barton and Choubey,<sup>8</sup> and Bandis et al.<sup>9</sup> proposed similar strength criteria, with a smooth transition between the two extreme types of response proposed by Patton.<sup>4</sup> Barton and Choubey,<sup>7</sup> and Bandis et al.<sup>8</sup> introduce the empirical coefficients JRC (Joint Roughness Coefficient) and JCS (Joint Compressive Strength) in their strength criterion. These empirical coefficients are easily determined either in the laboratory or in situ and they are a measure of the roughness of the joint surface (JRC) and the strength of the asperities (JCS). Empirical relations are proposed by these authors in order to include scale-dependency of JRC and JCS. The above strength criteria delineate the state of stress that separates pre-sliding and post-sliding of the joints. In order to predict the stress-strain behaviour of joints in both stages, numerous constitutive relationships have been proposed. These relationships could be categorized into two main classes. The incremental relationships<sup>10-15</sup> consist of piecewise linear relationships between the increment of stress and the increment of strain. These relationships are usually developed from direct shear tests under constant normal stress and their use under different load paths is not straightforward. Graphical methods to use these models to predict shear behaviour under constrained dilation (or constant normal stiffness) have been proposed with some success.<sup>16-18</sup> Boulon and Nova<sup>15</sup> and Benjelloun<sup>4</sup> proposed an incremental approach with directional dependency. In this approach, the stress-strain matrices are determined from elementary stress paths derived from laboratory tests (such as shear under constant normal stress conditions). A weighted interpolation procedure between the elementary stress paths is used to determine the incremental stress-strain matrix for other stress paths. The second category of constitutive relationships are the elastoplastic relationships, derived from the theory of plasticity. The models which fall into this category assume that before sliding, the deformations are elastic (recoverable). Post-sliding behaviour is characterized by plastic (irrecoverable) deformations. The state of stress that separates elastic from plastic behaviour is defined by appeal to a yield criterion. For example, Roberds and Einstein<sup>19</sup> used the strength criterion proposed by Patton<sup>5</sup> as the yield criterion to formulate their elastoplastic model. Strain-softening (decrease in shear stress in the plastic stage) often found in experimental behaviour of joints could not be predicted from the model proposed by Roberds and Einstein.<sup>19</sup> Numerous elastoplastic models exist in the literature (see, e.g. References 1 and 19, to name only some). The elastoplastic approach has a particular appeal since different load paths and directions could be accommodated. Among the above models, the one proposed by Plesha<sup>4</sup> is particularly attractive due to its simplicity and its ability to capture certain fundamental aspects of the mechanical behaviour of real joints, such as dilation under shear and strain softening due to surface asperity degradation.

For predicting the hydraulic behaviour of rock joints, the parallel plate model, developed from the application of the Navier-Stokes equation for laminar incompressible flow between two parallel smooth plates, is widely used to calculate the effective permeability of a fracture (see, e.g. Reference 4). The permeability of the joint is thus expressed as a function of its effective opening to fluid flow, called the hydraulic aperture. Since natural fractures are quite dissimilar to ideal parallel plates, the hydraulic aperture of the fracture is not equal to its mechanical aperture. Empirical relationships between the mechanical and hydraulic apertures were proposed by



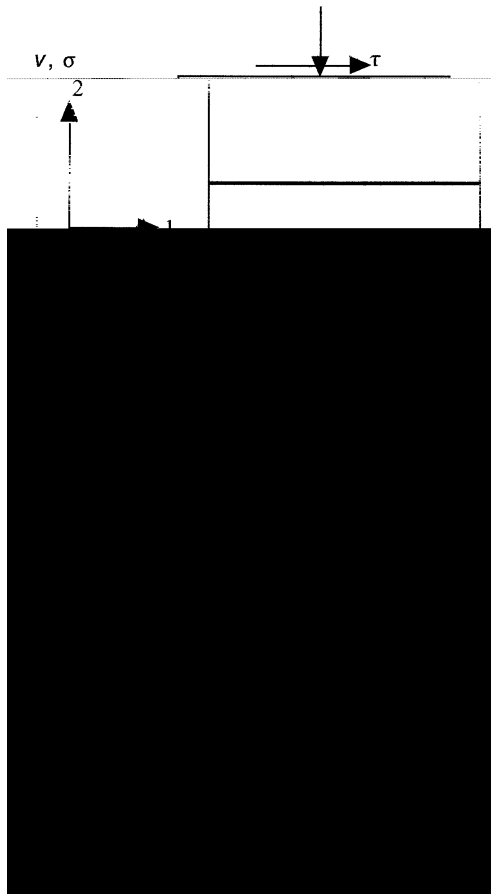


Figure 1. Joint model proposed by Patton

By imposing the constraint that only shear traction can produce permanent deformation due to sliding, Michalowski and Mroz proposed that, in the case of perfectly plane contact surface.

$$Q'' = |q| \quad (4)$$

In Patton's model shown in Figure 1, the asperities have regular angles of inclination with respect to the horizontal direction. Along a typical asperity inclined at angle  $\alpha$ , the relationship

and thus, the yield criterion for the saw-tooth joint model is

$$F = (p \sin \alpha + q \cos \alpha) \tan (\alpha + \phi) \quad (8)$$

Similarly, the plastic potential function is defined as

$$Q = (p \sin \alpha + q \cos \alpha) \quad (9)$$

Derivation of the elastoplastic stress matrix of the model by Plesha

In the formulation presented by Plesha, sliding along the asperities is considered. When the magnitude of the applied shear stress is such that, as defined in equation (8), is less than zero, only elastic deformations in the shear direction take place. Plastic or irrecoverable deformations in both shear and normal directions take place when  $F = 0$ . The total increment of relative displacement at the joint, in this case, is the sum of an elastic and a plastic component; i.e.

$$du = du^e + du^p \quad (10)$$

When plastic displacements occur, the asperities of the joint are damaged, resulting in a decrease of the asperity angle. Plesha assumes that the asperity angle decreases as an exponential function of the plastic work produced by shear

$$\alpha = \alpha_0 \exp \left( - \frac{1}{c} \int p \, du^p \right) \quad (11)$$

where  $\alpha_0$  is the original asperity angle,  $c$  is a degradation coefficient and  $\int p \, du^p$  is the plastic work produced by the shear stress

$$\int p \, du^p = \int p \, du - \int p \, du^e \quad (12)$$

where  $\int p \, du^e$  is the relative joint shear displacement.

From the consideration of asperity degradation, strain softening behaviour will now occur at the joint during plastic deformation, i.e. both the yield surface and the potential surface, as defined respectively, by equations (8) and (9), will shrink in the  $p$ - $q$  stress space. Both  $F$  and  $Q$  will now be functions of not only  $q$  and  $p$  but also of the plastic work defined by equation (12) (i.e.  $F = F(q, p, \int p \, du^p)$  and  $Q = Q(q, p, \int p \, du^p)$ ).

The increment of stress  $dp$  is related to the increment of elastic displacement at the joint by

$$dp = D \, du^e \quad (13)$$

where  $D$  is the elastic stiffness matrix (with elements having units of Pa/m in SI units).

Following conventional procedures applicable to the mechanics of elastoplastic solids and interface plasticity, it can be shown that

$$dp = D^* \, du \quad (14)$$

where  $D^*$  is the elastoplastic stiffness matrix, given by

$$D^* = D - \frac{1}{t} \frac{LQ}{H L_p} D \cdot D \cdot \frac{LF}{L_p} \quad (15)$$

and

$$j'' = \frac{1}{t!} \frac{LF}{H L_p} D_{\sim} du$$

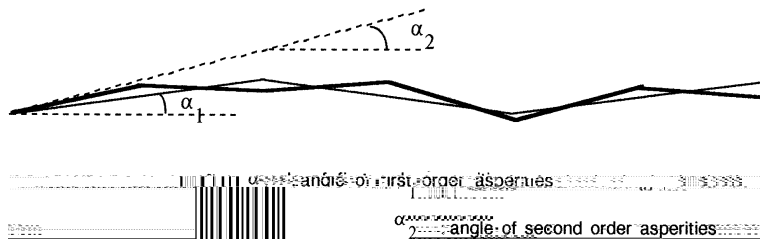


Figure 2. Schematic illustration of the many orders of asperities for real joints

The coefficients JRC (dimensionless) and JCS (MPa) and the friction angle can be easily estimated from two tests, the tilt test and the Schmidt hammer test. To determine  $\alpha$ , an artificial clean joint is prepared by diamond-sawing of a rock specimen containing the real joint, and sandblasting the surfaces. The jointed rock specimen is then tilted until sliding occurs along the clean joint. The tilt angle measured will be equal to  $\alpha$ . The angle  $\alpha$  reflects pure friction resistance of clean (unweathered) planar surfaces. The friction angle for the real joint also reflects pure frictional behaviour. Nevertheless, the real joint contains gouge material originating from the failure of surface asperities. From the results of 135 shear tests on natural joints, Barton and Choubey<sup>8</sup> have proposed the following empirical relationship between  $\alpha$  and  $\alpha_0$ , i.e.

$$\alpha = (\alpha_0 + 20) \# 20(r/R) \tag{22}$$

where, R and r are rebound value ( $\eta$ ) from the Schmidt hammer test performed, respectively, on a clean, dry unweathered surface and on a wet joint surface. JCS, the joint wall compressive strength is obtained from a simple empirical relation with the Schmidt rebound value

$$\log_{10} JCS = 0.00088R \# 1.601 \tag{23}$$

where JCS is in MPa,  $\rho$  is the unit weight of the dry rock in kN/m<sup>3</sup>.

The value of JRC, on the other hand, is determined from the tilt test, by using equation (19)

$$JRC = (b \# r) / \log(JCS / \rho_0) \tag{24}$$

where b is the tilt angle when sliding occurs and  $\rho_0$  is the self-weight induced normal stress acting on the joint, at the instant of sliding.

The parameters JRC and JCS are both scale-dependent. Bandis<sup>9</sup> proposed the following empirical relations:

$$JRC = JRC_0 \left( \frac{A}{B} \right)^{0.02 JRC} \tag{25}$$

$$JCS = JCS_0 \left( \frac{A}{B} \right)^{0.03 JRC} \tag{26}$$

where  $JRC_0$  and  $JCS_0$  are laboratory-scale values, for joints with normal size  $B_0 = 100$  mm and JRC and JCS are values for larger samples, of size

Bandis et al.<sup>9</sup> also experimentally observed that,  $\alpha_{1\%}$ , the shear displacement corresponding to the peak shear stress  $\sigma_{1\%}$ , under constant normal stress conditions, can be considered to be

independent of the normal stress but is scale dependent, i.e.

$$u_{1\%} = \frac{JRC}{500} \frac{p}{k_j} \tag{27}$$

Assuming linear elastic response of the joint up to the peak shear stress, we can obtain, from equations (19) and (27), the elastic shear stiffness as follows:

$$k_4 = \frac{dq_{1\%}}{du_{1\%}} = \frac{p \tan(JRC \log_{10} \frac{JCS(p)}{(\cdot/500)/(JRC/)} )}{(, /500)/(JRC/ )} \tag{28}$$

The remaining parameter required for the model proposed by Plesha is the normal stiffness  $k_j$ . This parameter can be determined by performing compression tests on jointed rock specimens. The most comprehensive experimental investigations on the normal closure behaviour of joints under applied normal stresses are due to Bandis et al. In these studies, 64 pairs of specimens, with a wide range of rock types and surface roughness were tested. Each pair of specimens consists of one jointed specimen and one unjointed specimen. Normal compression tests were performed on both specimens. The deformation of the unjointed specimen was subtracted from the deformation of the jointed specimen in order to obtain the net deformation properties of the joint. Typically, several cycles of loading/unloading were performed. Strong hysteresis is observed for the first few cycles and this hysteresis progressively disappears with the number of cycles. The third or fourth cycle is generally considered to be representative of *in situ* conditions. The normal stress-closure curves have the shape of steep hyperbolae. Several authors adopt hyperbolic relations to describe these experimental curves. For example, Bandis et al. proposed the following hyperbolic relationship:

$$p = k_{j*} \frac{v}{1 + v/v} \tag{29}$$

where  $k_{j*}$  is the normal stiffness at zero normal stress, and  $v$  is the maximum closure of the joint. The normal stiffness at any level of normal stress is then

$$k_j = \frac{dp}{dv} = k_{j*} \frac{p}{v \cdot k_{j*} \cdot p} \tag{30}$$

The parameters  $k_{j*}$  and  $v$  that enter into equation (30) are best determined by performing compression tests on jointed rock samples.

### HYDRAULIC BEHAVIOUR OF A JOINT

The parallel plate model, developed by the application of the Navier-Stokes equation for laminar incompressible flow between two parallel smooth plates, is usually used to calculate the permeability  $k$  of the fracture (see, e.g. Reference 4), i.e.

$$k = \frac{e^3}{12} \tag{31}$$

where  $e$  is the hydraulic aperture of the joint.

Since natural fractures are quite dissimilar to ideal parallel plates, the hydraulic aperture of the fracture is not equal to its mechanical aperture. Barton proposed the following empirical



relationship to estimate the hydraulic aperture from the mechanical aperture

$$e_h = \frac{e_m^2}{JRC^2} \quad (32)$$

where  $e_h$  is in l m,  $e_m$  (also in l m) is the mechanical aperture of the joint.

Elliot et al.<sup>25</sup> and Witherspoon et al.<sup>26</sup> proposed a linear relationship between the hydraulic and mechanical apertures

$$e_h = e_{h0} + f^* e_m \quad (33)$$

where  $e_{h0}$  is the initial hydraulic aperture,  $e_m^*$  is the variation in mechanical aperture due to the combined effects of compression and shear as discussed in the above section,  $f^*$  is a proportionality factor. Benjelloun<sup>4</sup> experimentally confirmed the validity of equation (33) and found that  $f^*$  varies between 0.5 to 1. This factor comes from the roughness of the joint surfaces. A factor  $f^* = 1$  applies to the limiting ideal case of parallel smooth plates; this situation prevails only when the joint is relatively open, with apertures of the order of mm. For most other cases,  $f^* < 1$ . The

## Shear under constant normal stress

Most laboratory experiments on joints are performed under constant normal stress conditions. These conditions apply mainly to geomechanical problems associated with rock slope stability, where the focus is on the analysis of the sliding movement of rock blocks near the surface of a slope. The constant normal stresses across the joints between these blocks is due to the weight of the blocks themselves.

We show here the simulation of experiments involving shear under constant normal stress performed by Skinaset al.<sup>18</sup> The tests were conducted on 15 cm x 10 cm model joints. These

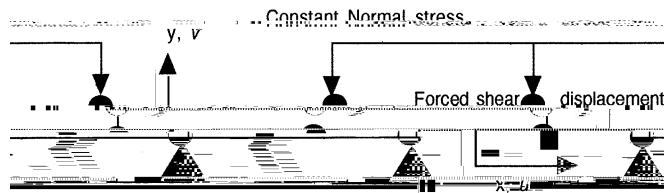


Figure 4. Finite element model for joint shear under constant normal stress condition

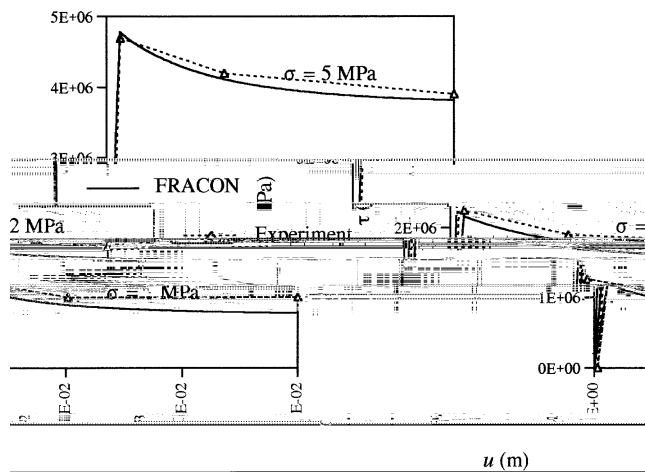


Figure 5. Shear under constant normal-stress shear stress vs. shear displacement

The results for shear stress versus shear displacement are shown in Figure 5. A close fit was obtained between the results derived from the numerical modelling and the experimental results. Figure 5 shows that the shear strength of the joint increases with the normal stress level, at the same time the joint becomes more brittle (i.e. strain softening becomes more pronounced). The displacement corresponding to the peak shear stress does not depend on normal stress level, but only on the size of the joint sample [cf. equation (31)]. These observations are also consistent with experimental results obtained by other researchers (e.g. References 4, 8, 9).

The joint dilation due to shear is shown in Figure 6. For a value of the normal stress of 1 MPa, the FRACON code overpredicts dilation by approximately 15 per cent when compared to the experimental results. This might be due to an inherent feature of the implementation of the model by Plesha into the FRACON code. This model does not allow the joint surfaces to approach one another as the asperities are degraded. Plesha included this damage deformation in a recent version of his model. The FRACON code nevertheless correctly predicts decreasing dilation with increasing normal stress, as found experimentally by numerous researchers (e.g. References 4, 8, 9). No experimental data were given by Skinaet al.18 for dilation at normal stress values of 2 MPa and 5 MPa.

Figures 7 and 8 illustrate the effects of degradation on the joint behaviour, for a typical case (normal stress of 1 MPa). From Figure 7, it may be observed that the joint would behave in an

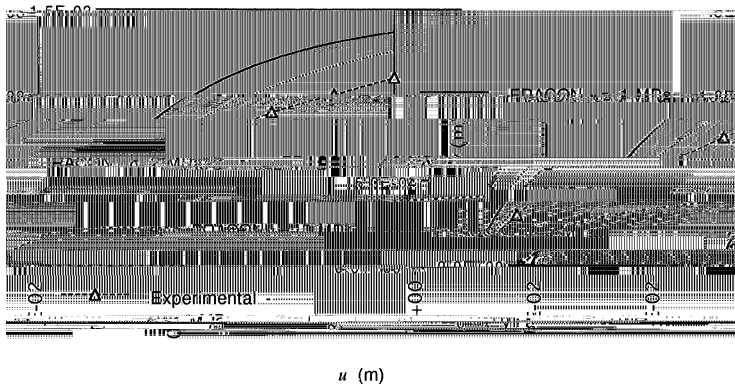


Figure 6. Shear behaviour under constant normal stress conditions

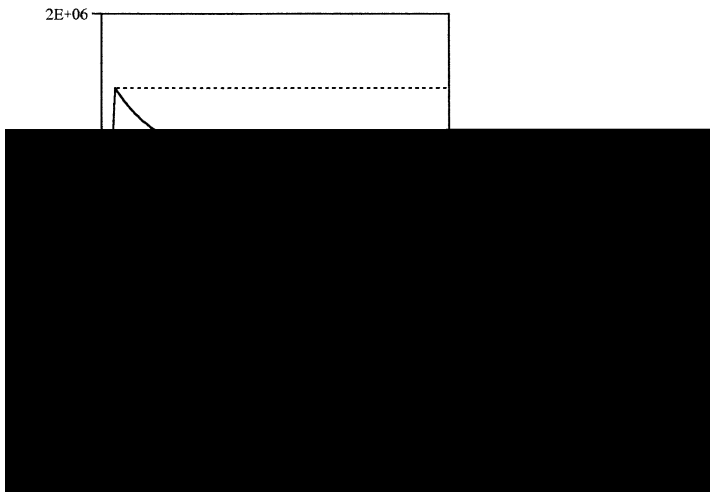


Figure 7. Effects of degradation on shear stress

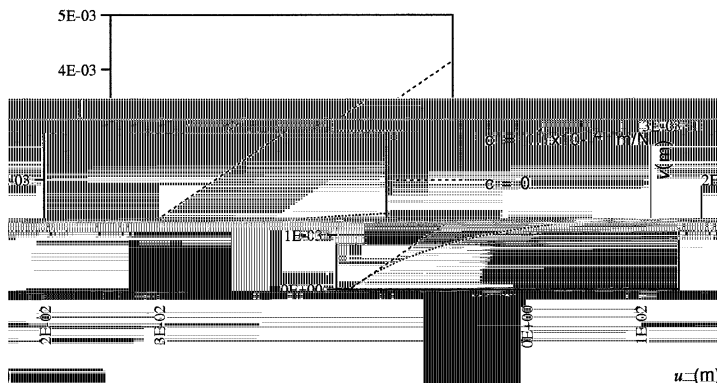


Figure 8. Effects of degradation on dilation

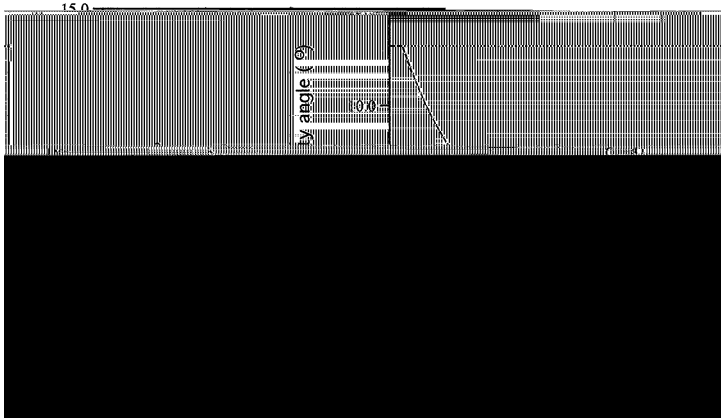
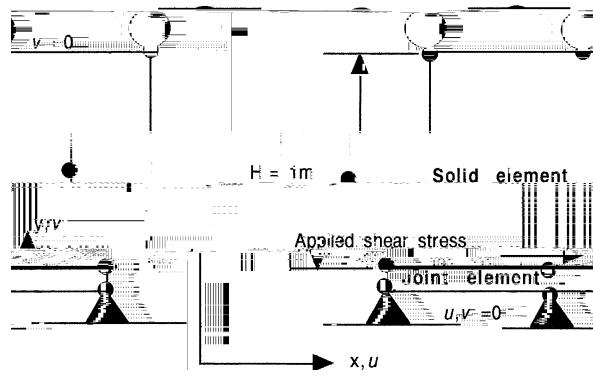


Figure 9. Effects of degradation on the asperity angle

elastic



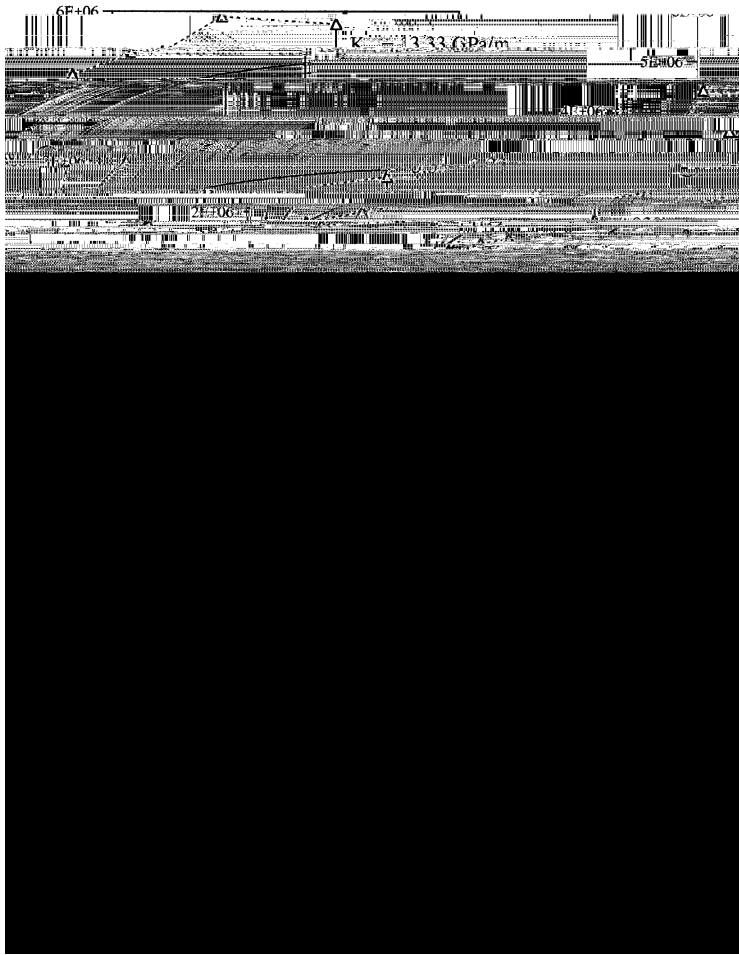


Figure 11. Joint behaviour under constant normal stiffness conditions

a corresponding increase in the permeability of the joint (Figure 13). However, this permeability later decreases due to gouge production by joint asperity breakage. Bandis et al. (1980) could not simulate this permeability decrease (Figure 13), using Barton's (1976) model.

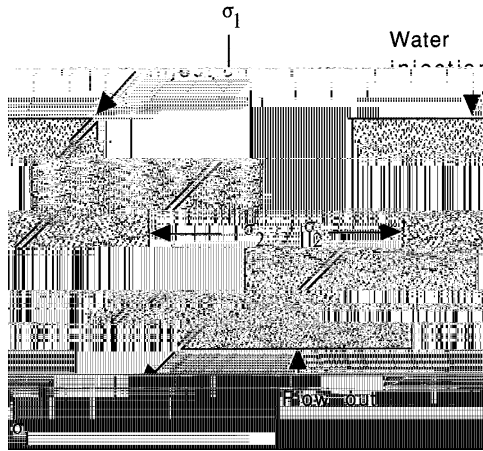


Figure 12. Schematics of the hydromechanical experiments performed by Bandis et al. 2 and Makurat et al. 3

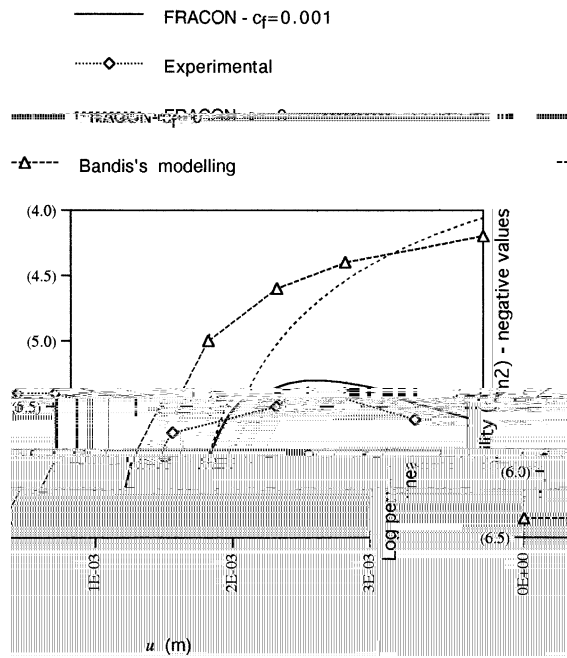


Figure 13. Hydromechanical experiments. Effects of shear on joint permeability

into smaller samples for testing separately. In these experiments shear tests were performed under constant normal stress conditions.

In this study, the scale effects in the tests conducted by Bandis et al. 9 are simulated by using the properties given in their studies:

$$d_0 = 6 \text{ cm} \quad JRC_0 = 16.7 \quad JCS_0 = 2 \text{ MPa} \quad \text{normal stress} = 24.5 \text{ kPa}$$



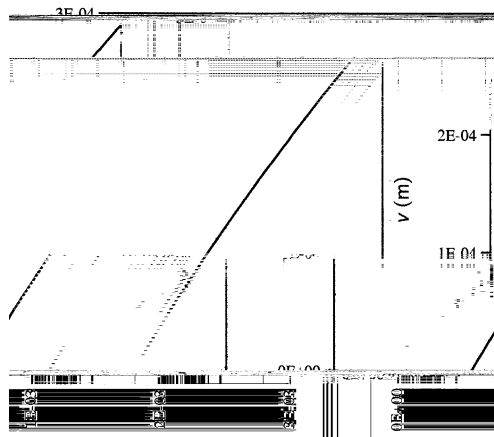


Figure 14. Hydromechanical experiments'shear dilation calculated via the FRACON code

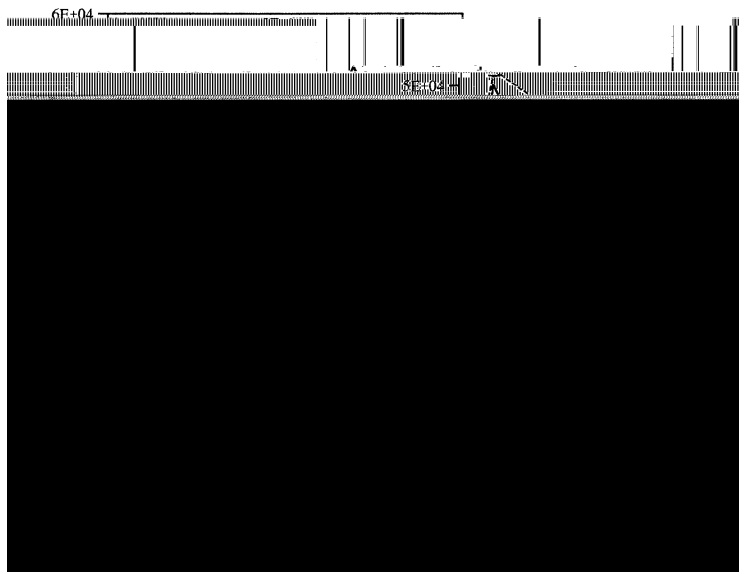


Figure 15. Scale effects on joint shear

Scale effects are simulated with the FRACON code by using the empirical equations (25) and (26). The finite element mesh used in the study is similar to the one shown in Figure 4.

Figure 15 shows that the FRACON code correctly predicts that with increasing size, strain softening is less pronounced, i.e. the joint behaviour becomes less brittle. With increasing size, the shear stiffness prior to failure decreases and the displacement required to reach the peak shear stress increases. The shear strength of the joint is somewhat underestimated by the numerical modelling, especially for the larger specimens.

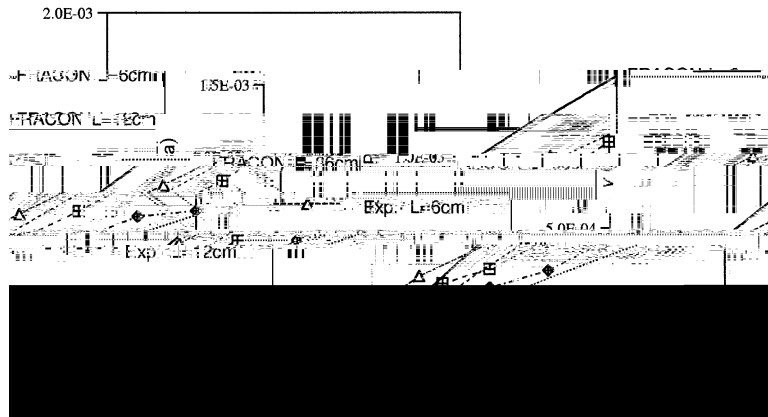


Figure 16. Scale effects on joint dilation

Figure 16 shows scale effects on joint dilation. The FRACTION code correctly predicts a decrease in shear dilation with larger samples. The experimental data shows that dilation starts before the peak shear stress is attained. As can be seen in Figure 16, the model by Pflüsch incorporated in the FRACTION code assumes linear elastic behaviour in the pre-peak phase. Thus, dilation is predicted to start only after the attainment of the peak shear stress. As previously discussed, because no damage deformation is incorporated in the model, with the smaller joint samples, the FRACTION code overpredicts the dilation value.

## CONCLUSIONS

A joint model was implemented in a finite element code (FRACTION) to simulate coupled thermal



14. W. Lechnitz, "Mechanical Properties of rock joints", *J. Rock Mech Min. Sci. Geomch Abst.*, 22, 313-321 (1985).
15. M. Boulon and R. Nova, "Modelling of soil-structure interface behaviour: A comparison between elastoplastic and rate type laws", *Comput Geotech*, 9, 21-46 (1990).
16. G. Archambault, M. Fortin, D. E. Gill, M. Aubertin and B. Ladanyi, "Experimental investigations for an algorithm simulating the effect of variable normal stiffness on discontinuities shear strength", *Proc. Int. Symp on Rock Joints*, Loen, Norway, Balkema, 14-18, 1990.
17. B. Amadei and S. Saeb, "Constitutive models of rock joints", *Proc. Int. Symp on Rock Joints*, Loen, Norway, Balkema, 70-72, 1990.
18. C. A. Skinas, S. Bandis and C. A. Demiris, "Experimental investigations and modelling of rock joint behaviour under constant stiffness", *Proc. Int. Symp on Rock Joints*, Loen, Norway, Balkema, 30-38, 1990.
19. W. J. Roberds and H. H. Einstein, "Comprehensive model for rock discontinuities", *Geotech Engng, Proc. ASCE*, 104, 553-569 (1978).
20. J. Ghaboussi, E. L. Wilson, and J. Isenberg, "Finite element for rock joints and interfaces", *Soil Mech Found Div. Proc. ASCE*, 99, 833-848 (1973).
21. K. Hsu-Jun, "Nonlinear analysis of the mechanical properties of joint and weak intercalation in rock", *Proc. 3rd Int. Conf on Num Methods in Geomechanics*, Aachen, Germany, 52-53, 1979.
22. G. N. Pande and W. Xiong, "An improved multilaminar model of jointed rock masses", *Numerical Models in Geomechanics*, A. A. Balkema, Rotterdam, 21-26, 1982.